SCIENTIFIC Publishing Limited

Prevention and Treatment of Natural Disasters

https://ojs.ukscip.com/index.php/ptnd/

Article

Flood Modeling and Emergency Planning for Dam Failure: Projections in Calabria (Italy)

Giandomenico Foti [1,*], Giuseppe Barbaro [1], Domenica Catalfamo [2], Antonino Siclari [2] and Giuseppe Bencivinni [2]

[1] DICEAM Department, Mediterranea University of Reggio Calabria, Reggio Calabria 89122, Italy
[2] Protection of the territory and the environment Section, Metropolitan City of Reggio Calabria, Reggio Calabria 89125, Italy
[*] Correspondence: giandomenico.foti@unirc.it;

Received: 30 July 2024; **Revised**: 13 August 2024; **Accepted**: 15 September 2024; **Published**: 30 September 2024

Abstract: A dam is a hydraulic structure made of natural materials, such as earth, or artificial ones, such as concrete, whose main function is to block a watercourse to create an artificial basin with multiple purposes, irrigation, energy, flow regulation, and protection. These structures allow for the storage of large quantities of water which, in the case of a collapse, can have devastating effects on human lives and territory. Therefore, the regulations prescribe severe safety checks and provide operational guidelines for civil protection activities and emergency plans. Through some case studies in Calabria, a region of Southern Italy, the paper analyzes Italian regulations concerning scenarios where it is necessary to safely empty the reservoir behind the dam following an earthquake and allow the consequent civil protection activities and emergency plans to be defined. Also, this paper describes the coupled hydrological and hydrodynamic modeling carried out using HEC-HMS and HEC-RAS, respectively, to define three thresholds for each dam according to Italian regulations. These thresholds are the maximum flow rate for emptying the dams that are contained in the hydraulic pertinence areas downstream of the dams, the attention flow rate for the discharge of the dam beyond which hydraulic criticalities occur, and the incremental thresholds that identify scenarios with greater hydraulic criticalities.

Keywords: Dam; Dam Failure; Civil Protection Activities; Emergency Plans; Floodable Areas; Modeling.

1. Introduction

A dam is a permanent artificial barrier designed to regulate the outflow of a natural watercourse or to form a reservoir for irrigation purposes, water supply, or to serve a hydropower plant [1]. The International Commission on Large Dams (ICOLD) World Register of Dams counted about 62,000 dams worldwide which is estimated to grow in the future [2]. Dams are critical infrastructures whose safety must be properly managed in response to the massive impact of possible destruction on the population and the environment. Dam failures are rare but can cause huge damage and loss of

life. A dam failure is a catastrophic type of structural failure, which in the worst-case scenario can be rapid, causing an uncontrolled release of impounded water or the likelihood of such an unchecked release [3-6]. Among the major dam failures of the past, it is worth mentioning Bouzey in Eastern France in 1895 with a failure sequence that comprised two phases: an initial break near the crest in the middle of the structure over a length of 20 m, followed by the main collapse of 180 m of the dam to a depth of about 10 m [7]; Gleno in the Central Italian Alps in 1923 that suddenly collapsed a few days after the first complete reservoir filling due to structural deficiencies [8]; St. Francis in Southern California in 1928 where immediately after the first complete filling of the reservoir, fractures and water leaks appeared on the face and abutments which, a few days later, extended to the base of the dam leading to its collapse [9]; Sella Zerbino in the Apennines of Northern Italy in 1935 due to an overtopping wave caused by an exceptionally severe rainfall where the flood exceeded the maximum capacity of the spillways and the bell valve was clogged up with sediments and debris [10], Niedow in Poland in 2010 due to a breach in the earth-type dam caused by an extreme rainfall with return period of over 100 years [11]. Another important event is that of Vajont (1963), where there was no collapse of the dam but a landslide from one of the slopes caused a wave that overtopped the dam, flooding the downstream territories [12,13].

From this point of view, a useful tool to mitigate the consequences of these floods is the perimeter of the floodable areas, especially if they involve anthropized areas. Therefore, many regulations prescribe severe safety checks and provide operational guidelines for civil protection activities and emergency plans in floodable areas [13]. Historical floods generated by dam failure have been widely analyzed and modeled [14,15]. Both one-dimensional and two-dimensional models are generally considered in modeling, depending on the goal of the analysis [16-20]. These models are useful to decision-makers for defining civil protection activities and emergency plans and managing areas flooded by the dam [21-23]. An accurate estimate of inundation altitudes and the arrival time of flood waves are important to consider when developing emergency plans.

Most of the scientific literature on dam failure mainly focuses on analyzing catastrophic events and defining emergency plans following events that have occurred or are related to design failure conditions. Very little research focuses on the emergency plans to manage dam emptying operations in advance for conditions such as earthquake safety of existing dams, as in this case study. For example, Zhou et al. [24] describe a risk analysis and emergency plans consequent to the barrier lake created by the Mw 6.5 earthquake in 2014, in Niulan River in southwest China. Azeez et al. [25] describe a dam break analysis and flood disaster simulation in the arid urban environment of Um Al-Khair Dam in Saudi Arabia. Latrubesse et al. [24] describe a dam failure with a catastrophic flood in 2018 in the Mekong Basin with fatalities and displaced thousands of people. Gaagai et al. [17] describe a risk analysis of dam-break flooding in a semi-arid montane area of Yabous Dam in Northeastern Algeria. Sarchani and Koutroulis [18] describe a probabilistic model of a dam breach flood for Valsamiotis Dam in Crete. Verma et al. [19] describe a dam break flow simulation model for preparing emergency action plans for Bargi Dam failure, in India. Modeling is also widely used, but mainly to analyze catastrophic events. For example, Eldeeb et al. [20] analyzed the Grand Ethiopian Renaissance dam failure using HEC-RAS to define flood inundation maps related to the failure.

The paper, through some case studies in Calabria, a region of Southern Italy, analyzes Italian regulations concerning civil protection activities and emergency plans related to dam failure and earthquake safety. Also, this paper describes the coupled hydrological and hydrodynamic modeling carried out using HEC-HMS and HEC-RAS, respectively, to define three thresholds for each dam according to Italian regulations. These thresholds are the maximum flow rate for emptying the dams that are contained in the hydraulic pertinence areas downstream of the dams QAmax, the attention flow rate for the discharge of the dams Qmin beyond which hydraulic criticalities occur, and the incremental thresholds ΔQ that identifies scenarios with greater hydraulic criticalities than Qmin.

2. Materials and Methods

2.1. Study Area Description

Calabria is a region in southern Italy that is an interesting case study because of its geomorphological, climatic, hydrological, and anthropic peculiarities.

About geomorphological peculiarity, most (over 90%) of the Calabrian territory is mountainous or hilly, and the rest is flat. The main massifs are the Pollino, the Sila, and the Aspromonte, located in the northern, central, and southern parts of Calabria, respectively, and all with a maximum altitude of about 2000 m. About the climatic peculiarity, Calabria has a notable variability with a mountain climate in the inland areas, with frequent rainfall and snowfall, and a Mediterranean climate along the coasts. The average annual rainfall is about 1100 mm, which varies from 1400 and 1800 mm in mountainous and from 500 and 1000 mm along the coast. Regarding the hydrological peculiarity, most Calabrian rivers, also called fiumare, have a hydrological regime, such as that of ephemeral rivers, that convey flow only during a rainfall event [27-30]. Regarding the anthropic peculiarity, in the latest 70 years in Calabria, considerable anthropic pressure has been observed, with the expansion of inhabited centers also close to rivers and coasts and often in a disorganized and unplanned way [31-38].

The analyzed dams are all located in the central-southern part of Calabria and are those of Lordo, within the Lordo River basin, Menta, within the Amendolea River basin, and Metramo, within the Mesima River basin (**Figure 1**). Menta and Metramo dams are in mountain areas far from the river mouth. In the first case, the river downstream of the dam does not cross inhabited centers, while the town of Galatro is crossed in the second case. Instead, the Lordo dam is located just 3 km upstream from the river mouth, close to the town of Siderno and there were no tributaries downstream of the dam.

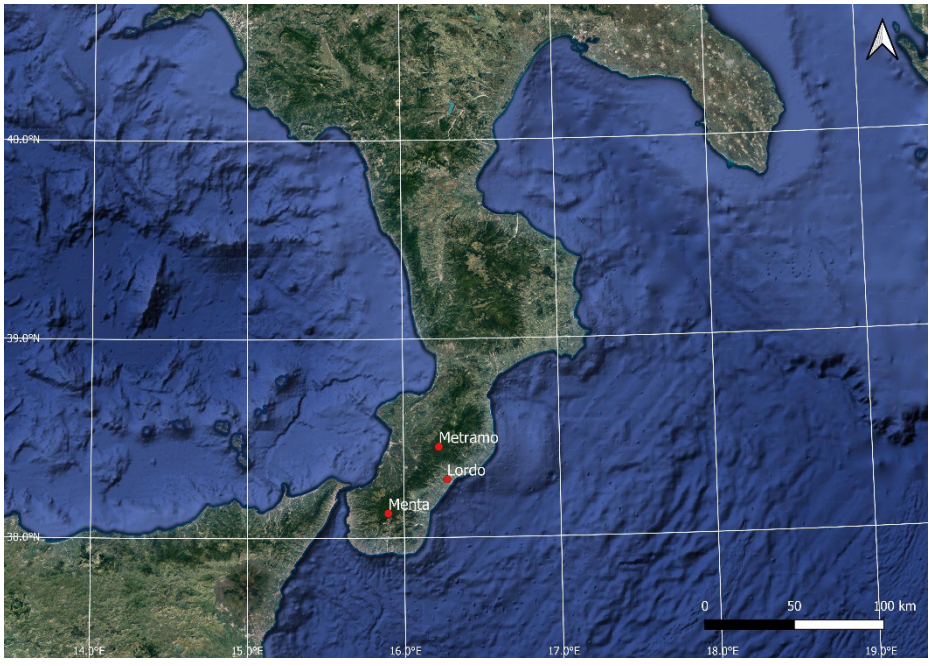

Figure 1. Location of the analyzed dams.

2.1.1. Lordo Dam

The Lordo Dam is located at an altitude of just under 100 m, a few kilometers upstream from the town of Siderno, and the outlets are directly connected to the main stream. The dam has a reservoir area of 0.7 km^2, is of the zoned type,

and is made up of loose materials. The central core is made of sandy clay with silt. The counter-cores and the filters, inserted between the core and the counter-core, are made of alluvial material from the riverbed. The upstream face is covered with limestone rocks while the downstream face is covered by grassy turf.

The dam height is over 40 m, and the crest is about 8.5 m wide and over 600 m long. The upstream face has slopes between 2.3 and 3.5 % while the downstream face has slopes between 1.85 and 2.5 %. The dam has two outlets, including one surface and one bottom. The surface outlet is of the cup type with a diameter of 24 m and can drain at a flow rate of 220 m^3/s. The bottom outlet has three sections: entrance, tunnel, and mouth. The entrance can drain at a flow rate of over 120 m^3/s and consists of a circular pipe with a diameter of 3.8 m, a length of over 200 m, and a slope of 1%, operating mainly under pressure. Between the entrance and the tunnel, there are two rectangular gates measuring 2.4 x 3 m. The tunnel has a diameter of 3.9 m, a length of over 4500 m, and a slope of 2% with free surface operation. At the mouth, there are two dissipation basins, connected to the Lordo River via a canal.

2.1.2. Menta Dam

The Menta dam is in the Aspromonte National Park at an altitude of over 1400 m, and the outlets are directly connected to the main stream. The dam has a reservoir area of 0.8 km^2 and is part of the Menta water scheme consisting of an intake structure, diversion tunnel, penstock, hydroelectric power station, and water purification plant. It is about 90 m high, is made up of rockfill, and has a rectilinear main body and a lower extension on the right bank, with a circular shape and concavity towards the mountain, which closes a saddle located at a lower height than that planned for the reservoir.

The dam has three outlets, including one surface, one bottom, and one of exhaustion. The surface outlet is of the free threshold type with a length of 60 m and can drain at a flow rate of about 220 m^3/s. The bottom outlet can drain at a flow rate of 120 m^3/s and consists of a circular pipe with a diameter of 4.3 m and a length of about 500 m. Before arriving at the tunnel, water must pass two rectangular gates measuring 1.7 x 2.2 m.

2.1.3. Metramo Dam

The Metramo Dam is located at an altitude of over 800 m, and the outlets are connected to the Metramo River, a tributary of the Mesima River, whose confluence is more than 20 km downstream. The dam has a reservoir area of 1 km^2, which is of the zoned type and made up of loose materials. The central core is made of sandy silt. The counter-cores and the filters, inserted between the core and the counter-core, are made of alluvial material from the riverbed and rockfill. The upstream face is covered with large rocks while the downstream face is covered by grassy turf.

The dam height is over 90 m, the crest is about 10 m, and the 7-meter safety clearances were applied between the crest and the maximum level of the reservoir, due to the great height and high seismicity of the site. The upstream face has slopes between 2.15 and 3.5 while the downstream face has slopes of 1.9. The dam has three outlets, including one surface, one bottom, and one of exhaustion. The surface outlet is of the cup type with a diameter of 18 m and can drain at a flow rate of 380 m^3/s. The bottom outlet consists of a circular pipe with a length of about 600 m and a slope of 2.5%. Before arriving at the tunnel, water must pass two rectangular gates measuring 2.1 x 1.5 m. The exhaustion outlet consists of a circular pipe with a length of over 900 m.

2.2. Overview of Regulations

The most recent regulation by the Italian authority about the safety of the dams and the management of downstream hydraulic risk is from the Directive of the President of the Council of Ministers of 2014 [39]. The main aim is to define the conditions for activating the alert phases for the dams' safety and for managing the hydraulic risk, the actions following the activation of these phases also identifying the decision-makers. To do this, the regulation identifies the

functional and procedural links between the various decision-makers, the main one being Civil Protection, and indicates the drafting criteria for the Civil Protection Document, which is the reference framework for drafting the emergency plan for the territories downstream of the dam. This document contains information on the location and characteristics of the dam, the characteristics of the catchment area related to the dam, the characteristics of the reservoir (detention volume, operating, and maximum water levels, threshold values), and the municipality in floodable areas downstream of the dam. Regarding the threshold values, the Civil Protection Document defines three thresholds for each dam, QA-max, Qmin, and ΔQ. QAmax is the flow rate value that allows the safe emptying of the dam, for example following an earthquake, without flooding the downstream areas or with flooding contained within the areas mapped as risk areas or attention areas by the Basin District Authorities. The Water Directive 2000/60 of the European Parliament and of the European Council abolished the previous Authorities at regional and basin levels and established 110 Basin District Authorities at the European level, seven of which are in Italy and Calabria falls within the Southern Apennines Basin District Authority, which includes all Southern Italy. The Floods Directive 2007/60 of the European Parliament and of the European Council defines the procedure for drafting the Flood Risk Management Plan (Italian acronym PGRA, "Piano di Gestione del Rischio Alluvione"). This plan is drafted by each Basin District Authority and contains the mapping of the risk and attention areas. QAmax is related only to the characteristics of the dam discharges and does not consider any contemporary rainfall events. Instead, Qmin is an indicator of the occurrence of fixed event scenarios (such as localized flooding downstream of the dam) and considers the flow rates that can be generated by the catchment area downstream of the dam. Finally, the incremental thresholds ΔQ are values that are added to Qmin and are related to scenarios like those related to Qmin.

2.3. Methodology

The methodology was divided into three phases: morphometric, hydrological, and hydrodynamic modeling.

In the first phase, the morphometric modeling was carried out using the open-source software QGIS 3.10.7 'A Coruna' and the free software HEC-HMS 4.10 to perimeter and morphometric characterize basins and main sub-basins. The perimeter of basins and sub-basins was carried out using the GIS tools of HEC-HMS, starting from the Digital Terrain Model (DTM) and Digital Surface Model (DSM) First and Last with 1 m and 2 m grid resolution available in the Italian Geoportal (http://www.pcn.minambiente.it/mattm/progetto-pst-dati-lidar). The pre-processing of the DTMs and DSMs and the morphometric characterization of basins and sub-basins were carried out using QGIS, starting from the shapefiles of basins and sub-basins, obtained with the GIS tools of HEC-HMS, the hydrographic network and the lithological map shapefiles available in the Open Data section of the Calabrian Geoportal (http://geoportale.regione.calabria.it/opendata), and of the Corine Land Cover fourth level of 2018, available in the Open Data section of Higher Institute for Environmental Protection and Research, were used (https://groupware.sinanet.isprambiente.it/uso-copertura-e-consumo-di-suolo/library/copertura-del-suolo/corine-land-cover/corine-land-cover-2018-iv-level). In this phase we are computing the following properties: area; perimeter; lengths of the hydrographic network and the main stream; maximum and average heights; average slope; concentration-time [40-42]; Curve Number (CN), associating a CN value with each land use and soil type categories.

The hydrological modeling phase was carried out using HEC-HMS to estimate the flow rate with fixed return time in basins and sub-basins, useful to define the rainfall scenarios downstream of each dam and modeled in the following phase. The return times chosen were 2, 5, 10, 15, 25, 50, 75, 100, and 200 years to consider frequent and extreme events. The input data for this phase is the maximum annual rainfall recorded by the rain gauges in the basins, available in the Calabrian Multi-Risk Functional Center (http://www.cfd.calabria.it/). Each rain gauge's influence area was estimated on QGIS using the Thiessen polygon method [43]. The hydrological modeling was carried out using the Soil Conservation

Service (SCS) Curve Number methods to estimate net rainfall, SCS Unit Hydrograph to model the flood formation process, and Lag to model the flood propagation process, with Lag time equal to 60% of the mean concentration-time. In addition, Frequency Storm to model the rainfall regime was used, defined starting from rainfall-duration curves obtained through statistical analysis of the maximum annual values of rainfall data.

The hydrodynamic modeling phase was carried out using the HEC-RAS 6.4.1 free software and its RAS Mapper application to define the QAmax, Qmin, and ΔQ thresholds. The model of each study area was defined starting from the DTM and DSM mentioned above. On this general basis, detailed data from plano-altimetric surveys and design documents of bridges and hydraulic works were added, where available. The current conditions of the riverbed and the existing structures were verified by analyzing the high-resolution satellite images given by Bing, obtained through the panoramic view function, the most recent satellite images of Google Earth, and the images of Google Street View. Manning coefficients were chosen from Chow's tables [44] assuming the following values: 0.05 for Left Overbank (LOB), Channel, and Right Overbank (ROB) of the meandering natural sections, 0.04 for Left Overbank (LOB), Channel, and Right Overbank (ROB) of the meandering natural sections with sparse vegetation, 0.035 for LOB, Channel, and ROB of the straight natural sections, 0.035 for LOB, Channel, and ROB of the straight natural sections with sparse vegetation, 0.02 for LOB and ROB of the artificial embanked sections. The contraction and expansion coefficients were assumed to be equal to 0.1 and 0.3, respectively, for the sections distant from the bridges and equal to 0.3 and 0.5 for the sections immediately upstream and downstream of the bridges. As for boundary conditions, Critical Depth was chosen upstream, related to the outflow from the dam outlets, and known water surface equal to 0.5 m downstream, to conservatively consider a possible sea level increase caused by a sea storm concomitant with river flow. In summary, the Lordo model has a length of over 3 km and has 63 cross-sections and 4 bridges. Instead, the Menta model has a length of over 30 km and has 302 cross-sections, 4 bridges, and 2 check-dams, while the Metramo model has a length of over 120 km and has 564 cross-sections, 17 bridges, and 28 check-dams.

3. Results

3.1. Morphometric Modeling

The Lordo River basin (**Figure 2**) has an area of about 13 km^2 and it has not been divided into sub-basins because almost the entire basin belongs to the dam and the basin downstream of the dam, up to the mouth, has a narrow and elongated shape without tributaries. This basin has a perimeter of over 20 km, a length of hydrographic network of about 60 km, a main stream length of about 10 km, a maximum height of 600 m, an average height of 200 m, an average slope of 15%, a concentration-time of about 1.2 hours and a CN of 82. The Lordo River downstream of the dam has a length of just over 3 km and an average slope of just over 1%. The first 300 m of the river has a trapezoidal section, with a bottom slope of about 0.2%. The next part is meandering with thick shrubby vegetation and local accumulations of gravelly and sandy material. The final part is covered in concrete and is delimited by embankments of a height of about 3 m.

The Amendolea River basin (**Figure 3**) has an area of about 150 km^2 and has been divided into 11 sub-basins. This basin has a perimeter of about 70 km, a length of hydrographic network of about 420 km, a main stream length of over 40 km, a maximum height of over 1800 m, an average height of about 850 m, an average slope of about 30%, a concentration-time of over 2.3 hours and a CN of 77. The Amendolea River basin has a narrow and long shape with numerous small tributaries, and the dam is one of them in the mountainous part. The most important tributaries are Vallone Colella, Vallone Furria, Vallone Cremasto, Fiumara Condofuri, and Torrente Menta, the one where the dam is located. This river is entirely natural, predominantly meandering, except the final straight and embanked part, and is characterized by thick vegetation in the mountainous part, up to the confluence with the Vallone Colella, while the downstream part has

no vegetation.

Figure 2. Lordo River basin.

The Mesima River basin (**Figure 4**) has an area of about 800 km^2 and has been divided into 17 sub-basins. This basin has a perimeter of about 240 km, a length of hydrographic network of 850 km, a main stream length of over 50 km, a maximum height of about 1300 m, an average height of over 400 m, an average slope of over 15%, a concentration-time of about 5.3 hours and a CN of 76. This river basin has a rounded shape with numerous large tributaries. The most important tributaries are Fiume Potamo, Fiume Fermano, Torrente Sciarapotamo, Fiume Vacale, Torrente Anguilla, and Fiume Metramo, and the dam is in the last one, which flows into the Mesima about 20 km upstream from the river mouth. Therefore, this portion of the basin upstream of the confluence has been divided into just 3 sub-basins with an area between 150 and 220 km^2. This river is entirely natural, predominantly meandering, except the final straight part, and is characterized by thick vegetation especially in the Metramo River, except the part that passes through the town of Galatro where there is sparse vegetation with large rocks and there are about thirty check dams. Finally, most of the river is embanked, except the mountainous stretch between the dam and the town of Galatro.

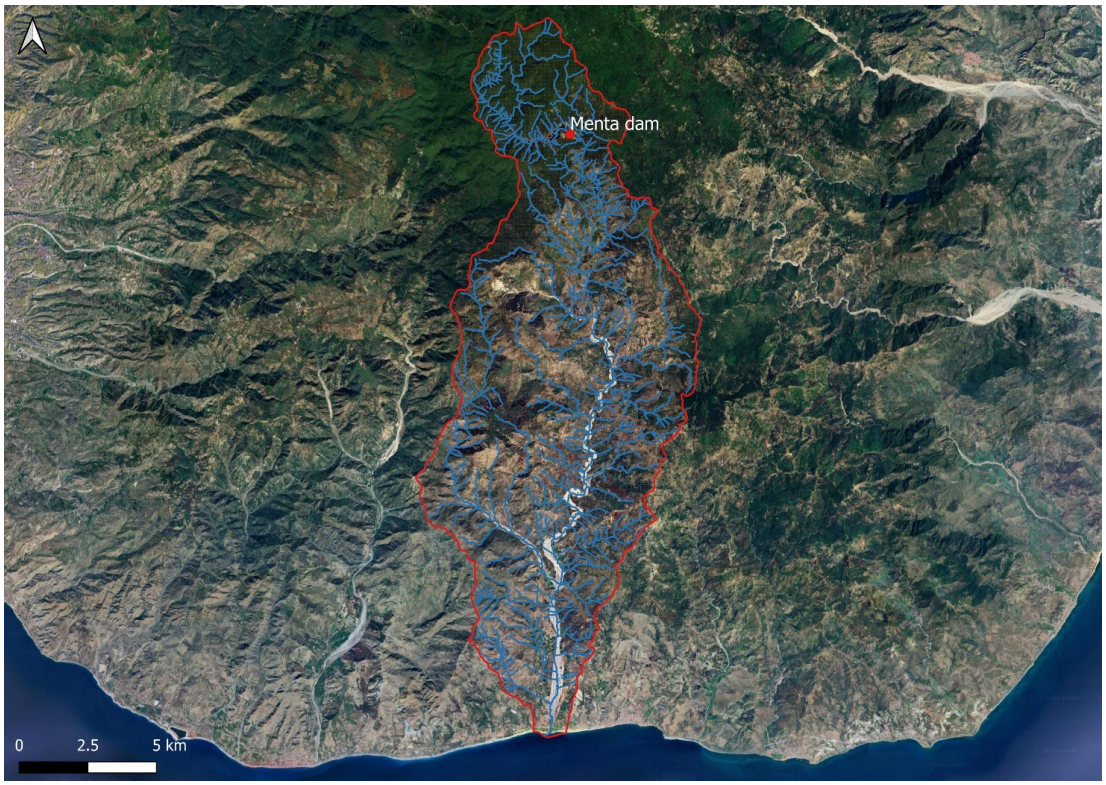

Figure 3. Amendolea River basin.

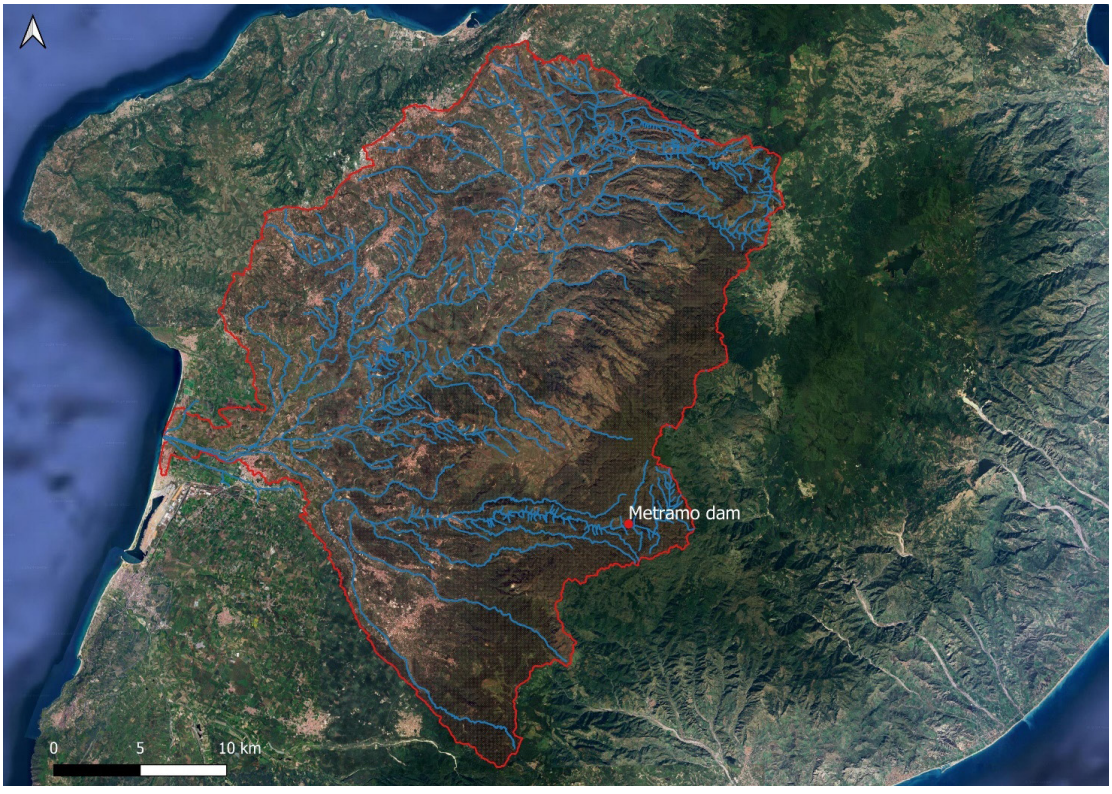

Figure 4. Mesima River basin.

Table 1 shows the main results of the morphometric modeling of the three basins.

Table 1. Main results of the morphometric modeling for each river basin. Legend: A area; P perimeter; L length of the hydrographic network; La length of the main stream; Hmax maximum height; Hav average height; I average slope; tc concentration-time; CN Curve Number.

Dam	Basin	A [km^2]	P [Km]	L [km]	La [lm]	Hmax [m]	Hav [m]	i [%}	tc [h]	CN
Lordo	Lordo	13.1	20.5	58.8	9.6	601	200	15	1.18	82
Menta	Amendolea	149.9	98	419.1	42.5	1830	845	26	2.48	77
Metramo	Mesima	791.1	236.3	850	54.2	1278	408	16	5.28	76

3.2. Hydrological Modeling

The hydrological modeling phase was carried out to estimate the flow rate with fixed return time (2, 5, 10, 15, 25, 50, 75, 100, and 200 years to consider frequent and extreme events) in basins and sub-basins, useful to define the rainfall scenarios downstream of each dam. As described above, the Lordo dam is located just 3 km upstream from the river mouth, close to the town of Siderno, and almost the entire river basin belongs to the dam and there are no tributaries downstream of the dam. Therefore, the hydrological rainfall scenarios were not computed in the hydraulic modeling.

In the Lordo River basin, the flow rates vary between 60 and 260 m^3/s; Amendolea River basin, the flow rates vary between 460 and 1760 m^3/s; in the Mesima River basin, the flow rates vary between 1300 and 7000 m^3/s.

Table 2 shows the flow rate with fixed return time (2, 5, 10, 15, 25, 50, 75, 100, and 200 years to consider frequent and extreme events).

Table 2. Values of flow rate with fixed return time (2, 5, 10, 15, 25, 50, 75, 100, and 200 years) for each river basin.

Dam	Basin	Q2 [m^3/s]	Q5 [m^3/s]	Q10 [m^3/s]	Q15 [m^3/s]	Q25 [m^3/s]	Q50 [m^3/s]	Q75 [m^3/s]	Q100 [m^3/s]	Q200 [m^3/s]
Lordo	Lordo	63.6	106.6	135.8	152.4	173.0	200.6	216.7	228.0	255.4
Menta	Amendolea	460.5	747.6	944.8	1057.5	1197.9	1387.3	1497.7	1575.9	1764.3
Metramo	Mesima	1287.7	2491.9	3355.1	3855.6	4485.4	5341.5	5843.5	6200.2	7062

3.3. Hydrodynamic Modeling and Floodable Areas

The hydrodynamic modeling was carried out considering the maximum flow rate for emptying the dams that are contained in the hydraulic pertinence areas downstream of the dams QAmax, the attention flow rate for the discharge of the dams Qmin, and the incremental thresholds ΔQ (see **Table 3**). In addition, some hydrological scenarios where the rainfall scenarios with return periods of 2, 5, 10, 15, 25, 50, 75, 100, and 200 years are added to the QAmax threshold were considered.

The QAmax flow rate downstream of the Lordo dam occurs without flooding in the final part of the river, close to the town center and protected by embankments (**Figure 5**). The passage under the bridges occurs with safety clearances of the order of 2 m, which are higher than the regulatory limits. Instead, in the meandering part, some sections at risk of flooding are, all falling within attention areas of the PGRA. In this part, there are mainly agricultural lands with a few isolated houses, generally located at higher altitudes than those reached by the water levels. Regarding other thresholds, Qmin occurs without flooding in any section while ΔQ identifies the start of flooding in the meandering part.

Table 3. Values of the maximum flow rate for emptying the dams that are contained in the hydraulic pertinence ar-

eas downstream of the dams QAmax, the attention flow rate for the discharge of the dams Qmin beyond which hydraulic criticalities occur, and the incremental thresholds ΔQ that identifies scenarios with greater hydraulic criticalities than Qmin for each analyzed dam.

Dam	QAmax [m^3/s]	Qmin [m^3/s]	ΔQ [m^3/s]
Lordo	220	40	70
Menta	78	30	50
Metramo	140	40	60

Figure 5. Floodable areas downstream of the Lordo dam related to QAmax.

The QAmax and Qmin flow rates downstream of the Menta dam occur without flooding Amendolea River (**Figure 6**) and the passage under the bridges occurs with safety clearances between 2 and 5 m, which are higher than the regulatory limits. Instead, in the ΔQ scenario, flooding is possible in the mountainous area immediately downstream of the dam, the confluence with the Vallone Colella. However, this is a non-anthropized area, characterized by steep slopes and thick vegetation. Once this threshold is exceeded, the area at risk of flooding increases significantly, especially in the mountainous part immediately downstream from the dam, before the confluence with the Vallone Colella. The hydrological scenarios where the rainfall scenarios with return periods of 2, 5, 10, 15, 25, 50, 75, 100, and 200 years are added to the QAmax threshold are characterized by 150 sections at risk of flooding, most of which (122) are in the mountainous part immediately downstream of the dam, before the confluence with the Vallone Colella. Of the remaining 28 sections, 12 are related to non-anthropized intermediate parts and 16 are related to the final anthropized part. In this last part, a

small village, some scattered houses, agricultural land, mining activities, and a coastal dune would be affected by the floods.

Figure 6. Floodable areas downstream of the Menta dam related to QAmax.

The QAmax and Qmin flow rates downstream of the Metramo dam occur without flooding the Metramo and Mesima rivers while downstream of Galatro the passage of QAmax occurs with only a few floods, are all located within attention areas of the PGRA that involve agricultural lands. The critical point is the upstream bridge inside Galatro town where the passage of QAmax under the bridges occurs with safety clearances of just 0.5 m, while the passage of Qmin under the bridges occurs with safety clearances of over 1.5 m. Instead, the ΔQ scenario was defined to obtain a safety clearance for the embankments of the order of one meter in all sections. The hydrological scenarios where the rainfall scenarios with fixed return periods are added to the QAmax threshold are characterized by various sections at risk of flooding. From this point of view, the greatest criticality is observed in the part of the river that passes through the town of Galatro. In fact, in this part, the QAmax passes without flooding. However, in the case of a concomitant hydrological scenario with a return period of 2 years, therefore a frequent scenario, to observe numerous sections at risk of flooding (**Figure 7**).

Figure 7. Floodable areas downstream of the Metramo dam related to Q2 scenario added to the QAmax threshold.

4. Discussion

The paper describes the methodology to define the QAmax, Qmin, and ΔQ thresholds, according to the Italian regulation. The first is the maximum flow rate for emptying the dams that are contained in the hydraulic pertinence areas downstream of the dams, and the second is the attention flow rate for the discharge of the dams beyond which hydraulic criticalities occur, and the last is the incremental threshold value that is added to Qmin and identifies scenarios with greater hydraulic criticalities than Qmin. These thresholds are related to scenarios where it is necessary to safely empty the reservoir behind the dam, for example following an earthquake, and allow the consequent civil protection activities and emergency plans to be defined. In addition to the indications of the Italian regulation, this paper analyzes some hydrological scenarios where the rainfall scenarios with return periods of 2, 5, 10, 15, 25, 50, 75, 100, and 200 years are added to the QAmax threshold. These scenarios, especially for extreme events, can significantly expand floodable areas, with the need to define specific control operations, as studied by Nakamura and Shimatani in Japan [45].

The methodology described in this paper can serve as a basis for defining emergency plans and developing flood forecasting models [46], such as what has been done by Pianforini et al. [47] for the Parma River dam. This methodology was applied in three dams of Southern Calabria, in Italy, very different from each other in terms of storage capacity, discharge capacity, size of the related river basins, and flow rates of these basins. The analyzed dams are those of Lordo, within the Lordo River basin, Menta, within the Amendolea River basin, and Metramo, within the Mesima River basin.

Menta and Metramo dams are in mountain areas far from the river mouth. In the first case, the river downstream of the dam does not cross inhabited centers, while the town of Galatro is crossed in the second case. Instead, the Lordo dam is located just 3 km upstream from the river mouth, close to the town of Siderno and there were no tributaries downstream of the dam.

The Lordo River basin has an area of just over 10 km^2, significantly smaller than Amendolea River basin, which is about 150 km^2, and especially the Mesima River basin, almost 800 km^2. These differences in size also lead to significant differences in terms of flow rate with fixed return time. The flow rate with a return time of 2 years varies between 60 m^3/s, in the Lordo River, 460 m^3/s, in the Amendolea River, and 1300 m^3/s, in the Mesima River, while the flow rate with a return time of 200 years varies between 260 m^3/s, in the Lordo River, 1760 m^3/s, in the Amendolea River, and 7000 m^3/s in the Mesima River. Instead, in terms of the QAmax threshold, the highest values are observed in the Lordo dam, 200 m^3/s, while for the Menta and Amendolea dams the values are about 80 and 140 m^3/s, respectively. This is explained by the fact that these thresholds are not related to the basin size but to the characteristics of the outlets. The QAmax values of the Menta and Metramo dams are much lower than their respective river basins' 2-year return time flow rates. Instead, the QAmax value of the Lordo dam is of the same order of magnitude as the 100-year return time flow rate of its river basin. Therefore, this high value is of the same magnitude as a very intense hydrological scenario, and this explains why it is associated with more sections at risk of flooding than the other two dams. However, these sections are all located in the meandering part and the floodable areas all fall within the areas of attention of the PGRA. In addition, these sections mainly involve agricultural lands with a few isolated houses, generally located at higher altitudes than those reached by the water levels while the anthropized part does not present any sections at risk due to the presence of the embankments. The QAmax value of the Menta dam creates some critical issues only in the mountainous area immediately downstream of the dam, but this is a non-anthropized area, characterized by steep slopes and thick vegetation, and does not create any further critical issues in the valley part. Instead, this part is affected by other hydraulic criticalities: ruins of check dams, embankment gaps, vehicular paths in the riverbed (panoramic views of a large part of the river are even available on Google Street View), narrowing of the riverbed near a small town, with a width reduction from 400 to 100 m, mining activities in the riverbed, excessive sediment deposits [48]. Instead, the most critical condition in terms of QAmax value concerns Metramo occurs when crossing Galatro town, a highly anthropized area where the river width is just a few meters and there are numerous bridges while downstream of Galatro the passage of QAmax occurs with only a few floods, all located within attention areas of the PGRA that involve agricultural lands. The passage of QAmax under the bridges occurs with safety clearances of just 0.5 m, while the passage of Qmin under the bridges occurs with safety clearances of over 1.5 m, and just the hydrological scenarios characterized by events with a return period of 2 years cause many sections to be at risk of flooding. All this occurs even though the QAmax is much lower than their respective river basin's 2-year return time flow rate. From this point of view, it should be noted that, unlike the outlets of the Lordo and Menta dams which are directly connected to their main streams, the outlets of Metramo dams are connected to the Metramo River, a tributary of the Mesima River, whose confluence is more than 20 km downstream. Consequently, the portion of the Mesima River basin relating to the part of the Metramo River upstream of Galatro town alone has an area of just 40 km^2 and the flow rates vary from 350 and 1000 m^3/s with return periods of 2 and 200 years respectively, much lower than those of Mesima River basin.

5. Conclusions

The paper, through some case studies in Calabria, a region of Southern Italy, analyzes Italian regulations concerning scenarios where it is necessary to safely empty the reservoir behind the dam, for example following an earthquake, and allow the consequent civil protection activities and emergency plans to be defined.

This analysis mainly highlighted that coupled hydrodynamic-hydrological modeling carried out using HEC-HMS and HEC-RAS, respectively, is essential to define the maximum flow rate for emptying the dams that are contained in the hydraulic pertinence areas downstream of the dams, the attention flow rate for the discharge of the dam beyond which hydraulic criticalities occur, and the incremental thresholds that identify scenarios with greater hydraulic criticalities according to Italian regulation.

In addition, this study also analyzes conditions with the rainfall scenarios downstream each dam is added to QA-max, even though they are not required by the regulation. These scenarios allow the identification of potentially floodable areas and the definition of emergency plans if it is necessary to empty the dam during rainfall events.

Author Contributions

Conceptualization, G.F., G.Ba., D.C., A.S. and G.Be.; methodology, G.F. and G.Ba.; software, G.F.; validation, G.F., G.Ba., D.C. and A.S.; formal analysis, G.F. and G.Ba.; investigation, G.F.; resources, G.F., A.S. and G.Be.; data curation, G.F.; writing—original draft preparation, G.F.; writing—review and editing, G.F.; visualization, G.F., G.Ba., D.C., A.S. and G.Be.; supervision, G.Ba. and D.C.; project administration, G.Ba. and D.C.; funding acquisition, G.Ba. and D.C. All authors have read and agreed to the published version of the manuscript.

Funding

This work was supported by the Metropolitan City of Reggio Calabria.

Institutional Review Board Statement

Not applicable.

Informed Consent Statement

Not applicable.

Data Availability Statement

Publicly archived datasets analyzed:

Italian Geoportal, DTM and DSM section (http://www.pcn.minambiente.it/mattm/progetto-pst-dati-lidar)

Calabrian Geoportal, Open Data section (http://geoportale.regione.calabria.it/opendata)

Higher Institute for Environmental Protection and Research, Open Data section (https://groupware.sinanet.isprambiente.it/uso-copertura-e-consumo-di-suolo/library/copertura-del-suolo/corine-land-cover/corine-land-cover-2018-iv-level)

Calabrian Multi-Risk Functional Center (http://www.cfd.calabria.it/)

New data are unavailable due to privacy concerns.

Conflicts of Interest

The authors declare no conflict of interest.

References

1. Chen, J.; Shi, H.; Sivakumar, B.; Peart, M.R. Population, water, food, energy and dams. Renewable Sustainable Energy Rev 2016, 56, 18–28. [CrossRef]
2. Zarfl, C.; Lumsdon, A.E.; Berlekamp, J.; Tydecks, L.; Tockner, K. A global boom in hydropower dam construction. Aquat Sci 2015, 77, 161–170. [CrossRef]
3. Cenderelli, D.A. Floods from natural and artificial dam failures. In Inland Flood Hazards: Human, Riparian and Aquatic Communities; Wohl, E.E. Eds; Cambridge University Press: Cambridge, England, 2000; pp. 73–103. [CrossRef]
4. Luino, F.; Tosatti, G.; Bonaria, V. Dam failures in the 20th century: nearly 1000 avoidable victims in Italy alone. J. Environ. Sci. Eng. 2014, 3, 19–31.[CrossRef]
5. Zhang, L.; Peng, M.; Chang, D.; Xu, Y. Dam Failure Mechanisms and Risk Assessment; John Wiley & Sons: pHoboken, New Jersey, USA, 2016; pp. 307–321. [CrossRef]
6. Bonomelli, R.; Farina, G.; Pilotti, M.; Molinari, D.; Ballio, F. Historical comparison of the damage caused by the propagation of a dam break wave in a pre-alpine valley. J. Hydrol.: Reg. Stud. 2023, 48, 101467. [CrossRef]
7. Smith, N.A. The failure of the Bouzey dam in 1895. Construction Hystory 1994, 10, 47–65.[CrossRef]
8. Pilotti, M.; Maranzoni, A.; Tomirotti, M.; Valerio, G. 1923 Gleno dam break: Case study and numerical modeling. J. Hydraul. Eng. 2011, 137, 480–492. [CrossRef]
9. Begnudelli, L.; Sanders, B.F. Simulation of the St. Francis dam-break flood. J. Eng. Mech. 2007, 133, 1200–1212. [CrossRef]
10. Petaccia, G.; Lai, C.G.; Milazzo, C.; Natale, L. The collapse of the Sella Zerbino gravity dam. Eng. Geol. 2016, 211, 39–49. [CrossRef]
11. Kostecki, S.; Banasiak, R. The Catastrophe of the Niedów Dam—The Causes of the Dam's Breach, Its Development, and Consequences. Water 2021, 13, 3254. [CrossRef]
12. Vacondio, R.; Mignosa, P.; Pagani, S. 3D SPH numerical simulation of the wave generated by the Vajont rockslide. Adv. Water Resour. 2013, 59, 146–156. [CrossRef]
13. Ferrari, A.; Vacondio, R.; Mignosa, P. High-resolution 2D shallow water modelling of dam failure floods for emergency action plans. J. Hydrol. 2023, 618, 129192. [CrossRef]
14. Aureli, F.; Maranzoni, A.; Mignosa, P. A semi-analytical method for predicting the outflow hydrograph due to dam-break in natural valleys. Adv. Water Resour. 2014, 63, 38–44. [CrossRef]
15. Aureli, F.; Maranzoni, A.; Petaccia, G. Review of historical dam-break events and laboratory tests on real topography for the validation of numerical models. Water 2021, 13, 1968. [CrossRef]
16. Bharath, A.; Shivapur, A.V.; Hiremath, C.G.; Maddamsetty, R. Dam break analysis using HEC-RAS and HEC-GeoRAS: A case study of Hidkal dam, Karnataka state, India. Environ. Challenges 2021, 5, 100401. [CrossRef]
17. Gaagai, A.; Aouissi, H.A.; Krauklis, A.E.; Burlakovs, J.; Athamena, A.; Zekker, I.; Boudoukha, A.; Benaabidate L.; Chenchouni, H. Modeling and Risk Analysis of Dam-Break Flooding in a Semi-Arid Montane Watershed: A Case Study of the Yabous Dam, Northeastern Algeria. Water 2022, 14, 767. [CrossRef]
18. Sarchani, S.; Koutroulis, A.G. Probabilistic dam breach flood modeling: the case of Valsamiotis dam in Crete. Nat. Hazards 2022, 114, 1763–1814. [CrossRef]
19. Verma, S.; Sachin; Patra, K.C. Dam Break Flow Simulation Model for Preparing Emergency Action Plans for Bargi Dam Failure. In Hydrological Modeling: Hydraulics, Water Resources and Coastal Engineering; Jha, R., Singh, V.P., Singh, V., Roy, L.B., Thendiyath, R., Eds; Springer International Publishing: New York, USA, 2022; pp. 271–286. [CrossRef]
20. Eldeeb, H.; Mowafy, M.H.; Salem, M.N.; Ibrahim, A. Flood propagation modeling: Case study the Grand Ethiopian Renaissance dam failure. Alexandria Eng. J. 2023, 71, 227–237. [CrossRef]
21. Escuder-Bueno, I.; Serrano-Lombillo, A.; Fluixa-Sanmartin, J.; Morales-Torres, A. Evaluacion de la seguridad hidrologica de presas mediante modelos de riesgo simplificados. In: Risk Analysis, Dam Safety, Dam Security and Critical Infrastructure Management; Escuder-Bueno, I., Matheu, E., Altarejos-Garcia L., Castillo-Rodriguez J.T., Eds.; CRC Press: Leiden, Boca Raton, Florida, USA,2012; pp. 335–342. [CrossRef]
22. Wieland, M. Safety aspects of sustainable storage dams and earthquake safety of existing dams. Engineering 2016, 2, 325–331. [CrossRef]
23. Fluixá-Sanmartín, J.; Escuder-Bueno, I.; Morales-Torres, A.; Castillo-Rodríguez, JT. Comprehensive deci-

sion-making approach for managing time dependent dam risks. Reliab. Eng. Syst. Saf. 2020, 203, 107100. [CrossRef]
24. Zhou, X.; Chen, Z.; Yu, S.; Wang, L.; Deng, G.; Sha, P.; Li, S. Risk analysis and emergency actions for Hongshiyan barrier lake. Nat. Hazards 2015, 79, 1933–1959. [CrossRef]
25. Azeez, O.; Elfeki, A.; Kamis, A.S.; Chaabani, A. Dam break analysis and flood disaster simulation in arid urban environment: The Um Al-Khair dam case study, Jeddah, Saudi Arabia. Nat. Hazards 2020, 100, 995–1011. [CrossRef]
26. Latrubesse, E.M.; Park, E.; Sieh, K.; Dang, T.; Lin, Y.N.; Yun, S.H. Dam failure and a catastrophic flood in the Mekong basin (Bolaven Plateau), southern Laos, 2018. Geomorphology 2020, 362, 107221. [CrossRef]
27. Sabato, L.; Tropeano, M. Fiumara: a kind of high hazard river. Phys. Chem. Earth, Parts A/B/V]C 2004, 29, 707–715. [CrossRef]
28. Sorriso-Valvo, M.; Terranova, O. The Calabrian fiumara streams. ZfG 2006, 143, 109–125. [CrossRef]
29. Canale, C.; Barbaro, G.; Petrucci, O.; Fiamma, V.; Foti, G.; Barilla, G.C.; Puntorieri, P.; Minniti, F.; Bruzzaniti, L. Analysis of floods and storms: Concurrent conditions. Ital. J. Eng. Geol. Environ. 2020, 23–29. [CrossRef]
30. Canale, C.; Barbaro, G.; Foti, G.; Petrucci, O.; Besio, G.; Barillà, G.C. Bruzzano river mouth damage due to meteorological events. Int. J. River Basin Manage. 2022, 20, 499–515. [CrossRef]
31. Fiorini, L.; Zullo, F.; Marucci, A.; Romano, B. Land take and landscape loss: Effect of uncontrolled urbanization in Southern Italy. J. Urban Manage. 2019, 8, 42–56. [CrossRef]
32. Cantasano, N.; Pellicone, G.; Ietto, F. The coastal sustainability standard method: A case study in Calabria (southern Italy). Ocean Coast. Manage. 2020, 183, 104962. [CrossRef]
33. Bombino, G.; Barbaro, G.; D'Agostino, D.; Denisi, P.; Foti, G.; Labate, A.; Zimbone, S.M. Shoreline change and coastal erosion: The role of check dams. First indications from a case study in Calabria, southern Italy. Catena 2022, 217, 106494.[CrossRef]
34. Foti, G.; Barbaro, G.; Barillà, G.C.; Frega, F. Effects of anthropogenic pressures on dune systems—case study: Calabria (Italy). J. Mar. Sci. Eng. 2022, 10(1), article number 10. [CrossRef]
35. Foti, G.; Bombino, G.; D'Agostino, D.; Barbaro, G. The Effects of Anthropogenic Pressure on Rivers: A Case Study in the Metropolitan City of Reggio Calabria. Remote Sens. 2022, 14, 4781. [CrossRef]
36. Foti, G.; Scarascia Mugnozza, G.; Sicilia, C.L. Flood hazard analysis in the Oliveto River Basin (Southern Italy). Ital. J. Eng. Geol. Environ. 2022, 2, 5–15. [CrossRef]
37. Foti, G.; Barbaro, G.; Barillà, G.C.; Mancuso, P.; Puntorieri, P. Shoreline erosion due to anthropogenic pressure in Calabria (Italy). Eur. J. Remote Sens. 2023, 56, 2140076. [CrossRef]
38. Bombino, G.; Barbaro, G.; D'Agostino, D.; Denisi, P.; Foti, G.; Zimbone, S.M. Relationships between torrent check dam systems and shoreline dynamics in semi-arid Mediterranean area: A sub-regional focus in Calabria, Italy. Geomorphology 2024, 458, 109259. [CrossRef]
39. Official Journal of the Italian Republic. Available online: (accessed on 10 June 2024[CrossRef]
40. Giandotti, M. Previsione delle piene e delle magre dei corsi d'acqua. Memorie e studi idrografici. Servizio Idrografico Italiano, Report No 2, 1934. (in Italian).[CrossRef]
41. Kirpich, Z.P. Time of concentration of small agricultural watersheds. Civ. Eng. 1940, 10, 362.[CrossRef]
42. Natural Resources Conservation Service (NRCS). Available online: (accessed on 10 June 2024) .[CrossRef]
43. Williams, J.R.; Kannan, N.; Wang, X.; Santhi, C.; Arnold, J.G. Evolution of the SCS runoff Curve Number method and its application to continuous runoff simulation. J. Hydrol. Eng. 2012, 17, 1221–1229. [CrossRef]
44. Chow, V.T. Open-channel hydraulics, 1st ed.; Publisher: McGraw-Hill, New York, USA, 1959; pp. 1–680.[CrossRef]
45. Nakamura, R.; Shimatani, Y. Extreme-flood control operation of dams in Japan. J. Hydrol.: Reg. Stud. 2021, 35, 100821. [CrossRef]
46. Ma, H.; Fu, X. Real time prediction approach for floods caused by failure of natural dams due to overtopping. Adv. Water Resour. 2012, 35, 10–19. [CrossRef]
47. Pianforini, M.; Dazzi, S.; Pilzer, A.; Vacondio, R. Real-time flood maps forecasting for dam-break scenarios with a transformer-based deep learning model. J. Hydrol. 2024, 635, 131169. [CrossRef]
48. Foti, G.; Barbaro, G.; Manti, A.; Foti, P.; La Torre, A.; Geria, P.F.; Puntorieri P.; Tramontana, N. A methodology to evaluate the effects of river sediment withdrawal: The case study of the Amendolea River in southern Italy. Aquat. Ecosyst. Health Manage. 2020, 23, 465–473. [CrossRef]

Copyright © 2024 by the author(s). Published by UK Scientific Publishing Limited. This is an open access article under the Creative Commons Attribution (CC BY) license (https://creativecommons.org/licenses/by/4.0/).

Publisher's Note: The views, opinions, and information presented in all publications are the sole responsibility of the respective authors and contributors, and do not necessarily reflect the views of UK Scientific Publishing Limited and/or its editors. UK Scientific Publishing Limited and/or its editors hereby disclaim any liability for any harm or damage to individuals or property arising from the implementation of ideas, methods, instructions, or products mentioned in the content.